Compact wavelength division multiplexers and demultiplexers

Revital Shechter, Yaakov Amitai, and Asher A. Friesem

Compact devices for wavelength division multiplexing and demultiplexing, believed to be novel, are presented. These devices are based on planar optics configurations, comprising multiplexed diffractive optical elements. The principle, design, and recording of these planar devices are described, including the fact that the recording is done at a single wavelength in the green region. Experimental procedures and results for planar devices that can handle three wavelengths in the visible as well as in the near infrared are presented. © 2002 Optical Society of America

OCIS codes: 050.1970, 050.1950, 050.7330, 060.4230, 060.1810.

1. Introduction

Wavelength division multiplexing (WDM) and wavelength division demultiplexing (WDDM) are undoubtedly needed to increase the information-carrying capacity of fiber telecommunication systems. With these techniques, a large number of communication channels can be transmitted simultaneously over a single fiber. To implement WDM and WDDM, several devices and configurations have been developed, which include waveguides,[1,2] planar waveguides,[3] free-space interconnects,[4] volume holograms in Littrow configurations,[5] diffractive optical elements (DOEs),[6] and substrate mode grating structures.[7–9] Here we present a relatively simple and robust device for implementing WDM and WDDM, which is based on a planar optics configuration in which several DOEs, each a simple reflection linear grating, are recorded on a single substrate. A basic building block of the planar configuration is shown in Fig. 1. The configuration is composed of two identical DOEs, recorded on the same substrate, that act as reflection gratings. The gratings in Fig. 1 appear to act as transmission gratings, but this is not the case. The light that impinges on the first grating is reflected but is trapped inside the substrate by total internal reflection. The fibers are attached to a graded-index coupling lens, which is in turn attached to the DOE. The coupling lens collimates the light that emanates from the fibers, so that a collimated beam impinges on the first DOE. This first DOE diffracts the light coming from the fiber into the substrate at an angle higher than the critical angle, so that it is trapped inside the substrate. The light then travels inside the substrate by means of total internal reflection and impinges on the second DOE, which couples the light out of the substrate. The advantages of the proposed configuration are the relative simplicity of the design and recording of the elements, the compactness of the entire device, and its tolerances to changes in readout wavelengths and angle. A similar configuration was suggested for DOEs as transmission gratings.[10] Our approach, although more difficult to design and record, provides better spectral discrimination, leading to low cross-talk capabilities with more wavelength channels.

2. Basic Principles and Design Considerations

The basic planar configuration for a WDM and a WDDM that can handle n wavelength channels is shown schematically in Fig. 2. In this configuration, one main input DOE, comprised of n superimposed sub-DOEs, each a linear reflection grating designed for a specific wavelength, operates on n wavelengths, whereas the remaining output DOEs, each a single linear reflection grating, operates at a specific wavelength. For WDDM, the light from the input fiber that represents n communication channels, each with a different wavelength $\lambda_1, \lambda_2, \ldots, \lambda_n$, diffracted by each sub-DOE of the main DOE, so that it is trapped inside the substrate and the light of each wavelength is directed to a different direction. The light of each

R. Shechter (ferevita@wisemail.weizmann.ac.il), Y. Amitai, and A. A. Friesem are with the Department of Physics of Complex Systems, Weizmann Institute of Science, 76100 Rehovot, Israel.

Received 6 March 2001; revised manuscript received 16 August 2001.

0003-6935/02/071256-06$15.00/0

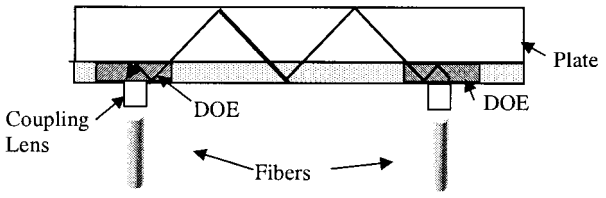

Fig. 1. Planar optics building block for a WDM system.

wavelength then travels in the substrate toward its respective output DOE, which diffracts it out into the output fiber. Evidently the propagation direction of the waves can be inverted to produce a WDM configuration, where light from the separated fibers is directed toward the central fiber. Since all the DOEs are recorded on the same thin substrate and the fibers can be attached to the substrate, the overall system can be compact and robust.

To obtain efficient light throughput and low cross talk between wavelength channels, each DOE must have a high diffraction efficiency for a specific wavelength λ_i and an as low as possible diffraction efficiency for all the other wavelengths. According to coupled-wave theory,[11] the diffraction efficiency η for a reflective linear grating, if we assume s polarization, is

$$\eta = \frac{1}{1 + \dfrac{1 - \xi^2/\nu^2}{\sinh^2\sqrt{\nu^2 - \xi^2}}}, \tag{1}$$

where ν and ξ are real-valued parameters that depend on the wavelength and geometry of the readout

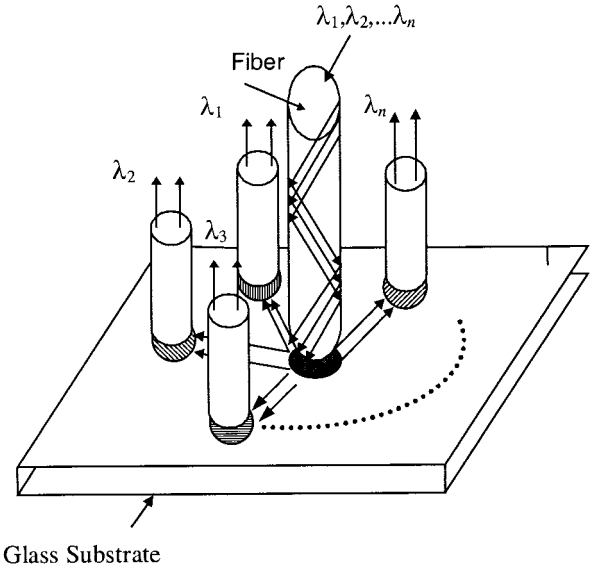

Fig. 2. Schematic configuration for a planar WDM or WDDM device.

illumination as well as on the parameters of the grating, for example,

$$\nu = \frac{i\pi\Delta n_i d}{\lambda_i(\cos\alpha_c \cos\alpha_d)^{1/2}}, \tag{2}$$

$$\xi = \frac{-\theta d}{2\cos\alpha_d}, \tag{3}$$

where $i = \sqrt{-1}$, Δn_i is the refractive-index modulation, d is the thickness of the recording medium, λ_i is the reconstruction wavelength, θ is the dephasing factor created by deviation from the Bragg condition, and α_c and α_d are the angular orientation of the readout and diffracted beams, respectively, inside the recording medium. The corresponding grating period is

$$\Lambda_i = \frac{\lambda_i}{2n\sin\dfrac{\alpha_d}{2}}. \tag{4}$$

To obtain high diffraction efficiency at the Bragg condition, for which $\xi = 0$, the value of ν should be as large as possible. One can obtain large values of ν by resorting to a recording medium of large thickness d or to a large refractive-index modulation Δn_i, both of which are limited in practice. For example, with our polymer materials, thickness d ranged from 20 to 80 μm, and the maximum refractive-index modulation $\Delta n_{\max}$ was 0.06.[12] Accordingly, to calculate the maximum number of wavelength channels, N_{chn}, that our planar configuration can deal with, we must first find the number of DOEs that can be superimposed in one location.[13] This depends on $\Delta n_{\max}$ and on the refractive-index modulation for each DOE Δn_i in accordance with

$$\sum_{i=1}^{N_{\text{chn}}} \Delta n_i \le \Delta n_{\max}. \tag{5}$$

Thus, for $\lambda_i = 1530$ nm, $d = 20$ μm, the desired diffraction efficiency of 90%, and an internal diffractive angle of 70 deg, we obtained $\Delta n_i = 0.0159$; the maximum allowed number of wavelength channels is $N_{\text{chn}} = \Delta n_{\max}/\Delta n_i = 3$. When d increased to $d = 80$ μm, we obtained $N_{\text{chn}} = 15$.

The number of wavelength channels and their separation also depend on thickness d of the recording medium. To determine the dependence of the number of wavelength channels on d we assume, for simplicity, that at the Bragg condition of $\xi = 0$, $\nu = \pi/2$, so the diffraction efficiency is 84%. Then Eq. (2) yields

$$\Delta n_i = \frac{-j\lambda_i\sqrt{\cos\alpha_d}}{2d}, \tag{6}$$

and we then obtain the number of wavelength channels from $N_{\text{chn}} = \Delta n_{\max}/\Delta n_i$. To determine the minimal separation between wavelength channels $\Delta\lambda$ at

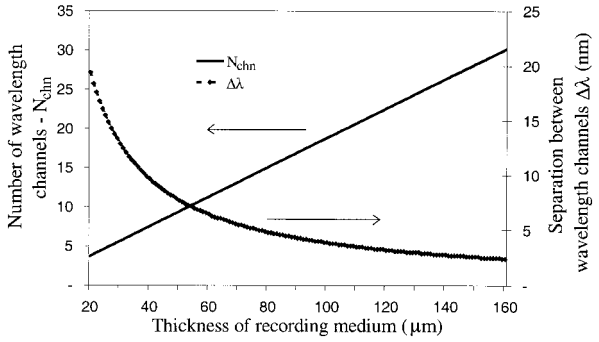

Fig. 3. Number of wavelength channels and their separation as a function of recording medium thickness d.

FWHM, we inserted Eq. (4) into Eqs. (1), (2), and (3), which yielded

$$\Delta\lambda_i = \pm \sqrt{1 + \frac{\nu_i^2}{\pi^2}} \frac{{\lambda_i}^2 \cos \alpha_d}{2nd \sin^2\left(\frac{\alpha_d}{2}\right)}. \quad (7)$$

As is evident from Eq. (7), the minimal separation $\Delta\lambda_i$ depends on ν_i, which in turn depends on Δn_i. If Δn_I is such that the diffraction efficiency of each DOE is 90%, according to Eqs. (1) and (2), when $\xi = 0$ we then obtain $\Delta\lambda_i = 5.33$ nm at $\lambda_i = 647$ nm for $d = 20$ μm and $\Delta n_i = 0.013$. At $\lambda_i = 1550$ nm we obtained $\Delta\lambda = 3.34$ nm for $d = 80$ μm and $\Delta n_i = 0.0016$. By use of the assumption that $\nu = \pi/2$, Eq. (7) reduces to

$$\Delta\lambda_i = \frac{\sqrt{5}{\lambda_i}^2 \cos \alpha_d}{4nd \sin^2\left(\frac{\alpha_d}{2}\right)}. \quad (8)$$

According to Eq. (8), we determined the number of wavelength channels that can be superimposed on the same area and the separation between them as a function of thickness d of the emulsion for $\lambda_i = 1530$ nm and an internal angle of 70 deg. The results are shown in Fig. 3. To conclude, increasing Δn_i results in higher light throughput efficiency but leads to fewer wavelength channels. Increasing the recording medium thickness d leads to a higher number of wavelength channels, since a smaller Δn_i is needed for the same diffraction efficiency, as well as to a smaller needed separation between these wavelength channels. For the simple DOEs in the planar configuration, we simply chose Δn_i to maximize the diffraction efficiency. For the multiplexed DOE, we optimized Δn_i to maximize the diffraction efficiency and the number of wavelength channels.

We calculated the diffraction efficiency as a function of wavelength for a simple DOE, assuming that the input light was s polarized. Some representative results are shown in Fig. 4. Figure 4(a) shows the diffraction efficiency as a function of wavelength for a planar DOE having the following parameters: $d = 20$ μm, $n = 1.51$, $\Delta n_i = 0.02$, $\lambda_l = 647$ nm, $\alpha_c = 0°$, $\alpha_d = 120°$. Figure 4(b) shows the results obtained for a planar DOE having the parameters:

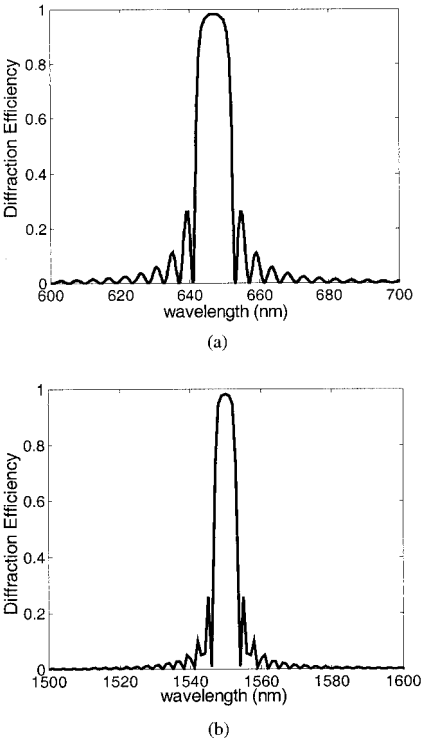

Fig. 4. Calculated diffraction efficiency as a function of wavelength for planar DOEs: (a) $\lambda_l = 647$ nm, $d = 20$ μm; (b) $\lambda_l = 1550$ nm, $d = 80$ μm.

$d = 80$ μm, $n = 1.51$, $\Delta n_i = 0.008$, $\lambda_l = 1550$ nm, $\alpha_c = 0°$, $\alpha_d = 100°$.

As is evident from these results, a separation of approximately 10 nm would be sufficient to obtain relatively low cross talk with only a 20-μm-thick recording medium at the visible wavelengths. The thickness must be increased to approximately 80 μm to obtain comparable separation at near-infrared wavelengths. When the input light is p polarized, the ν of Eq. (2) must be modified[11] to

$$\nu^p = \nu(\vec{r} \cdot \vec{s}) = \nu \cos(3\alpha_c + \alpha_d). \quad (9)$$

Accordingly, the diffraction efficiency for p polarization is different from that for s polarization. For example, using the same parameters as those used to obtain the results for Fig. 4(b), we calculated the diffraction efficiency for the p polarization to be only 20%.

One can achieve polarization insensitivity by resorting to one of the following two solutions. One possible solution is to increase the diffraction efficiency for p polarization to be as high as that for s polarization. This solution requires either higher-index modulation or a thicker recording medium. The disadvantages of this solution are fewer wavelength channels and increased sidelobes, resulting in high cross talk. The other solution is to orient the incident beam at a specific slant angle to the DOE. One can derive the needed exact orientation angle

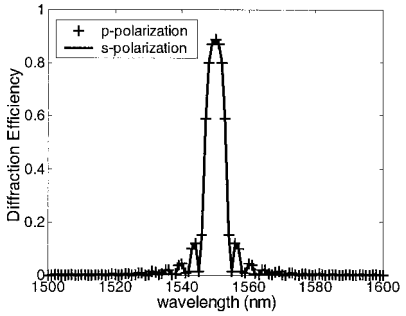

Fig. 5. Calculated diffraction efficiency as a function of wavelength for a planar DOE that is illuminated with an incident beam oriented at a slant angle $\lambda_l = 1550$ nm.

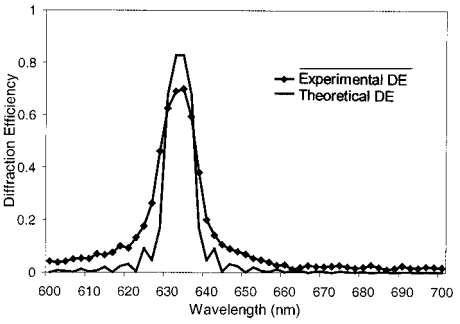

Fig. 6. Diffraction efficiency as a function of wavelength for a planar DOE designed to operate at $\lambda = 633$ nm.

from Eq. (9) by requiring that $\nu^p = \nu$. Accordingly, the preferred α_c in the substrate is

$$\alpha_c = -(\alpha_d/3). \tag{10}$$

Figure 5 shows the calculated diffraction efficiency for the two polarizations for $d = 80$ μm, $\Delta n_i = 0.005$, $\lambda_l = 1550$ nm, $\alpha_c = -35°$, and $\alpha_d = 105°$ (65° internal angle). As is evident, at a slant angle of 35 deg the DOE is essentially insensitive to the polarization of incident light. We note that this tilt angle depends only on the choice of internal angle, not on the wavelength, the thickness, or the modulation depth.

3. Experimental Results

To verify our design, we recorded two WDDM configurations for three wavelength channels: one for the visible wavelengths and the other for near-infrared wavelengths. Each configuration included six DOEs. Three were superimposed to form the central input DOE and the other three were the simple output DOEs that were laterally displaced from each other. For the WDDM that was used with visible wavelengths, the recording medium was a photopolymer with a thickness of 20 μm, and the other relevant parameters were $\Delta n = 0.011$, $\alpha_c = 0°$, and $\alpha_d = 120°$. The three wavelengths were $\lambda_1 = 633$ nm, $\lambda_1 = 647$ nm, and $\lambda_1 = 676$ nm. All the DOEs were recorded at $\lambda = 514.5$ nm so we had to adjust the recording geometry for each designed wavelength to obtain high diffraction efficiency.[14] Some representative results are presented in Figs. 6–9. Figure 6 shows theoretical and experimental spectral responses for one of the output DOEs designed for $\lambda = 633$ nm. Evidently there is a reasonable agreement between theory and experiment, especially for the spectral bandwidth and the operating wavelength. Figure 7 shows the theoretical and experimental angular responses for another DOE that was designed to operate at $\lambda = 676$ nm. As shown, there is good agreement between the angle and the maximal diffraction efficiency, although the experimental angular bandwidth is wider than that predicted. Figure 8 shows the experimental diffraction efficiency as a function of wavelength for the multiplexed input DOE. In this combined DOE the light diffracted from each sub-DOE propagates in a different direction. As expected, there are three peaks at the designed wavelengths. These experimental results reveal that the spectral bandwidths are somewhat larger than expected, and the diffraction efficiencies at the three wavelengths are not equal. These anomalies are probably due to variations of the recording parameters, which must still be optimized. We also determined the cross talk among the three wavelength channels by measuring the diffraction efficiency of each DOE for all three wavelengths. The results are summarized in Table 1, in which *m* denotes a multiplexed DOE and *s* denotes a single DOE.

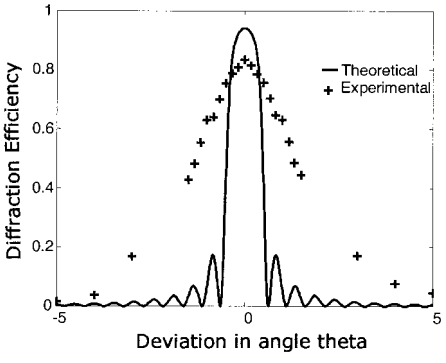

Fig. 7. Diffraction efficiency as a function of readout angle for a planar DOE designed to operate at $\lambda = 676$ nm.

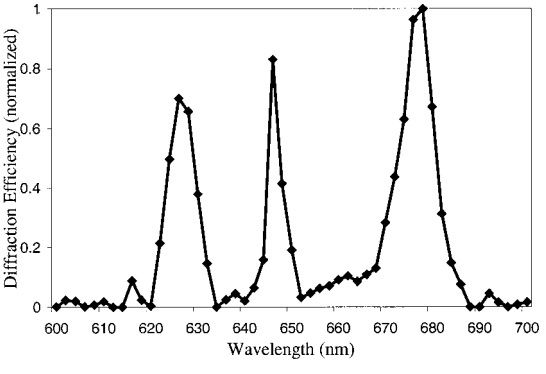

Fig. 8. Diffraction efficiency as a function of wavelength for a multiple input DOE.

Table 1. Diffraction Efficiency and Cross Talk of Each DOE for Three Visible Wavelengths[a]

Wavelength	DOE	Wavelength λ_1 (633 nm)	λ_2 (647 nm)	λ_3 (676 nm)
λ1 (633 nm)	*m*	70.0	0.9	0.1
	s	62.0	1.3	0.3
λ2 (647 nm)	*m*	0.8	83.0	0.5
	s	1.1	82.3	0.7
λ3 (676 nm)	*m*	0.0	0.7	96.0
	s	0.0	1.1	91.3

[a]*m*, multiplexed; *s*, single.

Finally, Fig. 9 depicts the overall performance of the full WDDM configuration, where the beams of each wavelength pass through the main input DOE and the corresponding output DOE. The cross talks for the full configuration are much lower. The highest cross talk of −29.3 dB was measured for the 633-nm wavelength channel when the readout beam wavelength was 647 nm. For all other cases the cross talk was lower than −40 dB. We note here that the uniform diffraction efficiency among the different wavelengths can be improved by optimization of the exposure procedure of the sub-DOEs.[13]

We also recorded a three-wavelength channel WDDM configuration for operation at the near-infrared wavelength. The parameters of the DOEs were the same as those used to obtain the results of Fig. 4(b), but the recording medium thicknesses d were 40 and 80 μm and Δn was around 0.006. The designed operating wavelengths were $\lambda_1 = 1510$ nm, $\lambda_2 = 1530$ nm, and $\lambda_3 = 1550$ nm. We again recorded all the DOEs at 514.5-nm wavelength with the recording geometry to achieve a high diffraction efficiency at the near-infrared wavelengths.[13] We determined that the DOEs had to be recorded as transmission DOEs at 514.5 nm to obtain reflection behavior in the near infrared.

Some representative results that show experimental and calculated diffraction efficiencies as a function of wavelength for specific DOEs are presented in Figs. 10 and 11. We observed good agreement between the experimental results and the calculated predictions. The slight wavelength shift is due to material shrinkage, a problem that we need to address by optimizing the preparation, recording, and development procedures. Figure 10 shows the results for a planar DOE designed to operate at λ = 1550 nm. The relatively high side fluctuations are due to instabilities of the readout laser, which was used initially. Figure 11 shows the results for a planar DOE designed to operate at λ = 1530 nm. Here a different, more stable, readout beam was used, resulting in lower side fluctuations. The spectral bandwidths were measured to give 6 nm for $d = 40$ μm and 3 nm for $d = 80$ μm.

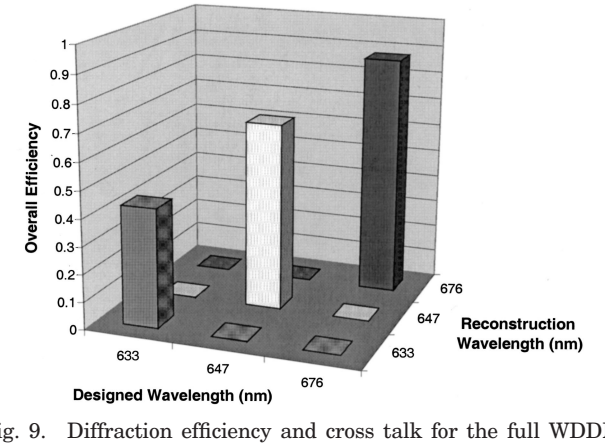

Fig. 9. Diffraction efficiency and cross talk for the full WDDM configuration with visible wavelengths.

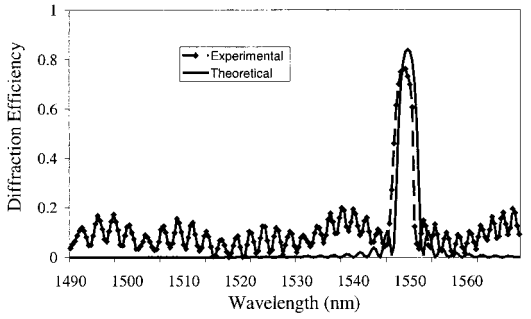

Fig. 10. Experimental and theoretical diffraction efficiency as a function of wavelength for a DOE designed to operate at λ = 1550 nm.

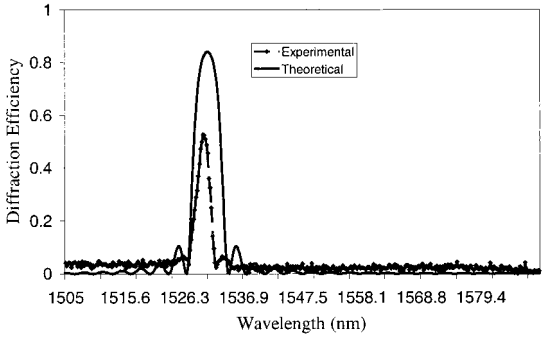

Fig. 11. Experimental and theoretical diffraction efficiency as a function of wavelength for a DOE designed to operate at λ = 1550 nm.

4. Concluding Remarks

We have presented a relatively simple, compact, and modular WDDM–WDM configuration that is based on planar optics. This configuration includes a multiplicity of DOEs that are recorded on thick recording materials. As the thickness of the recording material increases, it is possible to obtain relatively narrow spectral bandwidths, a larger number of wavelength channels, and relative cross talk.

This research was mainly supported by the PlanOp Company and partially by the Israel Ministry of Science.

References

1. A. Othonos, J. Bismuth, M. Sweeny, A. P. Kevorkian, and J. M. Xu, "Superimposed grating wavelength division multiplexing in Ge-doped SiO_2/Si planar waveguides," Opt. Eng. **37,** 717–720 (1998).
2. J.-F. Viens, C. L. Callender, J. P. Noad, L. A. Eldada, and R. A. Norwood, "Polymer-based waveguide devices for WDM applications," in *Organic Photorefractives, Photoreceptors, Waveguides, and Fibers*, S. Ducharme, D. H. Dunlap, and R. A. Norwood, eds., Proc. SPIE **3799,** 202–213 (1999).
3. V. Minier, A. Kevorkian, and J. M. Xu, "Superimposed phase gratings in planar optical waveguides for wavelength demultiplexing applications," IEEE Photon. Technol. Lett. **5,** 330–333 (1993).
4. M. Kajita, K. Kasahara, T. J. Kim, D. T. Neilson, I. Ogura, I. Redmond, and E. Schenfeld, "Wavelength-division multiplexing free-space optical interconnect networks for massively parallel processing systems," Appl. Opt. **37,** 3746–3755 (1998).
5. J. Liu and R. T. Chen, "Path-reversed substrate-guided-wave optical interconnects for wavelength-division demultiplexing," Appl. Opt. **38,** 3046–3052 (1999).
6. E. Pawlowski, M. Ferstl, H. Hellmich, B. Kuhlow, C. Warmuth, and J. R. Salgueiro, "Fabrication of a multichannel wavelength-division multiplexing-passive optical net demultiplexer with arrayed-waveguide gratings and diffractive optical elements," Appl. Opt. **38,** 3039–3045 (1999).
7. Y. K. Tsai, Y. T. Huang, and D. C. Su, "A reflection-type substrate-mode grating structure for wavelength-division-multi/demultiplexing," Optik (Stuttgart) **97,** 62–66 (1994).
8. Y. K. Tsai, Y. T. Huang, and D. C. Su, "Multiband wavelength-division demultiplexing with a cascaded substrate-mode grating structure," Appl. Opt. **34,** 5582–5588 (1995).
9. J. Liu and R. T. Chen, "Practical wavelength division demultiplexer for short-wavelength local area networks," in *Optoelectronic Interconnects VI*, J. P. Bristow and S. Tang, eds., Proc. SPIE **3632,** 273–284 (1999).
10. Y. Amitai, "Design of wavelength-division multiplexing/demultiplexing using substrate-mode holographic elements," Opt. Commun. **98,** 24–28 (1993).
11. H. Kogelnik, "Coupled wave theory for thick hologram gratings," Bell Syst. Tech. J. **48,** 2909–2948 (1969).
12. A. M. Weber, W. K. Smothers, T. J. Trout, and D. J. Mickish, "Hologram recording in du Pont's new photopolymer materials," in *Practical Holography IV*; *Proceedings of the Meeting, Los Angeles, CA, Jan. 18, 19, 1990*, S. A. Benton, ed., Proc. SPIE **1212,** 30–39 (1990).
13. S. H. Lin, K. Y. Hsu, W.-Z. Chen, and W.-T. Whang, "Exposure schedule for multiplexing holograms in photopolymer," in *Photorefractive Fiber and Crystal Devices: Materials, Optical Properties, and Applications V*, F. T. Yu and S. Yin, eds., Proc. SPIE **3801,** 100–106 (1999).
14. K. Winick, "Designing efficient aberration-free holographic lenses in the presence of a construction–reconstruction wavelength shift," J. Opt. Soc. Am. **72,** 143–148 (1982).